The advantages and disadvantages of bioorthogonal proteins

Groenewold, G.J.M.

Chapter 4

Exploring azido-HRP as a tool in immunocytochemistry

Abstract

Previously it was shown that horseradish peroxidase (HRP) could be modified with azide residues without losing its enzymatic activity. It was postulated that this modified protein could potentially be used as a new tool in immunocytochemistry. The production of this HRP-N_3 and its use as an enzymatic detection reagent for bioorthogonal groups was assessed, which proved to be useful for the detection of recombinant bioorthogonal proteins by dot blot and SDS-PAGE/Western blot, but not for the detection of bioorthogonal labels in an immunocytochemical setting.

Introduction

Immunohistochemistry and immunocytochemistry staining are well-established tools to visualize the presence of specific antigens in biological samples [1-3]. In these approaches, antibodies raised against antigens of interest conjugated to reporter proteins are used to detect their presence in tissue samples. Despite its long history, this process is still of pivotal importance in the clinic for the identification of primary tumors [4-6], pathogen infections [7-9], auto-immune disease [10-12] and other pathologies.

Paul Ehrlich is commonly regarded as the founding father of the fields of histochemistry and histopathology. His pioneering work on the use of aniline dyes on animal sections [13] allowed for the first time to directly visualize the presence of pathogenic bacteria in tissue samples [14]. In 1890 Emil von Behring reported on the harvesting and use of antibodies [15-17]. Marrack and co-workers subsequently and inspired by the work of Ehrlich and Behring came up with the idea to combine a dye with an antibody and in this manner color typhoid and cholera in tissue samples [18]. A decade later, Coons *et al.* performed what may be considered as the first true immunohistochemistry experiments by using antibody fluorophore conjugates to visualize pneumococci in histopathological samples [19]. Chemical conjugation of an antibody to reporter enzymes, technologies developed for the first time in the sixties of last century [20, 21], gave another major impetus to the field. Signal amplification, created through enzymatic processing of a reporter substrate, now allowed the detection of rare antigens. The use of substrate/enzyme pairs that yielded osmiophilic products, also allowed the combination of histochemistry with electron microscopy (EM)-based imaging techniques [1, 22].

Immunostaining thus pertains the formation of antigen-antibody complexes, and the subsequent detection of these complexes through visualizing the antibody that is selected and/or engineered for these purposes. The antigen-recognizing antibody can be directly conjugated to the reporter entity, for instance and as is depicted in Figure 1, horseradish peroxidase (HRP). Alternatively, the antigen-specific antibody may be designed such that it is recognized by a generic, secondary antibody that in turn is conjugated to HRP. In both these examples, antigens are detected by adding an HRP

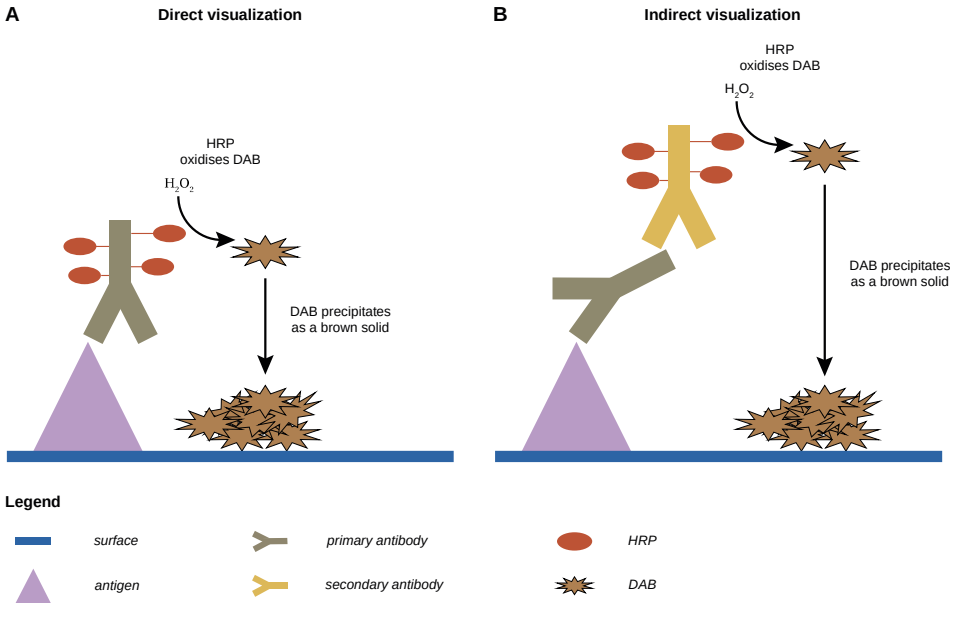

Figure 1. Different immunostaining approaches. A) Direct visualization of the antigen: The primary antibody, which recognizes a specific antigen, is conjugated to HRP. Hereafter HRP can precipitate for instance 3,3'-diaminobenzidine (DAB). B) Indirect visualization of the antigen: The primary antibody recognizes a specific antigen. The secondary will recognize this primary antibody and is conjugated to the visualization moiety, again used for DAB precipitation.

substrate that upon HRP-mediated oxidation yields a luminescent signal, or as depicted here, a colorimetric deposit.

Two of the used reporter enzymes are β-galactosidase (β-Gal) [23] and HRP [24]. When active, both can enzymatically convert so-called chromogens, compounds that produce a colored product. HRP, for example, can oxidize different substrates, such as 3,3'-diaminobenzidine (DAB) (Scheme 1A) [25, 26], 3-amino-9-ethylcarbazole (AEC) [27, 28] and 2,2'-azino-bis(3-ethylbenzothiazoline-6-sulphonic acid) (ABTS) (Scheme 1B) [29, 30], moreover it can oxidize chemiluminescent reagents such as luminol (Scheme 1C) [31]. The reactions as depicted in the forward direction in Scheme 1, are chemically as follows: 1. DAB reacts with H_2O_2 in the presence of the catalyst HRP. In the first step, a quinone iminium cation radical is formed after the donation of an electron to HRP, hereafter in the second step DAB polymerizes into a complex brown precipitate after the donation of another electron [32]. 2. The simplified reaction of 2 molecules of ABTS with H_2O_2 under the catalyzation of HRP resulting 2 ABTS radicals [33, 34]. 3. Luminol reacts

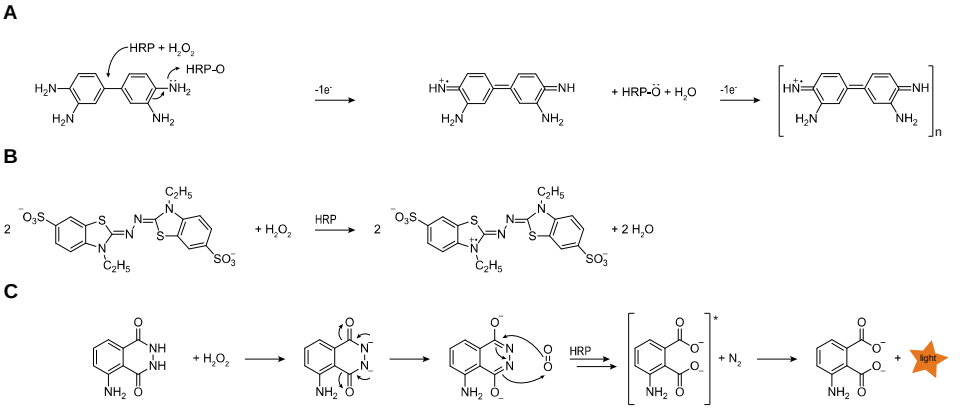

Scheme 1. Schematic overview of conversions by HRP. All of the here presented molecules react with H_2O_2 using HRP as a catalyst. A) DAB conversion into its insoluble brown precipitate. B) The formation of green ATBS radicals from ABTS. C) Oxidation of luminol resulting in luminescence.

with hydroxyl groups to form a dianion intermediate. After tautomerization and the reaction with hydrogen peroxide, an unstable peroxide is formed. The resulting compound, 3-aminophthalate, will be in its excited state and with the return to its ground state emit light [35, 36].

One caveat in immunohistochemistry is that certain antigens defy antibody recognition. Immunization of an antibody-producing host with small molecular antigens for instance and because of a limited number of chemical functionalities for antibody-antigen interaction, often yield low-affinity antibodies at most. Moreover, some antigens are simply not immunogenic, meaning no antibodies will be produced. Another caveat is the possible lack of specificity of an antibody towards the antigen it has been developed for, in which case cross-reactivity may yield false positives. Complementary histological techniques not reliant on antibodies or random chemical dye labelling could be an addition to further advance histological approaches.

One technique that has the potential to play a role in immunohistochemistry is bioorthogonal chemistry. With the introduction of this technique, it became possible to perform a chemical reaction in a biological setting without or with minimal interference of the natural processes in experimental settings [38]. In order to use bioorthogonal chemistry in an histochemistry approach, e.g. an azide group can be introduced into a

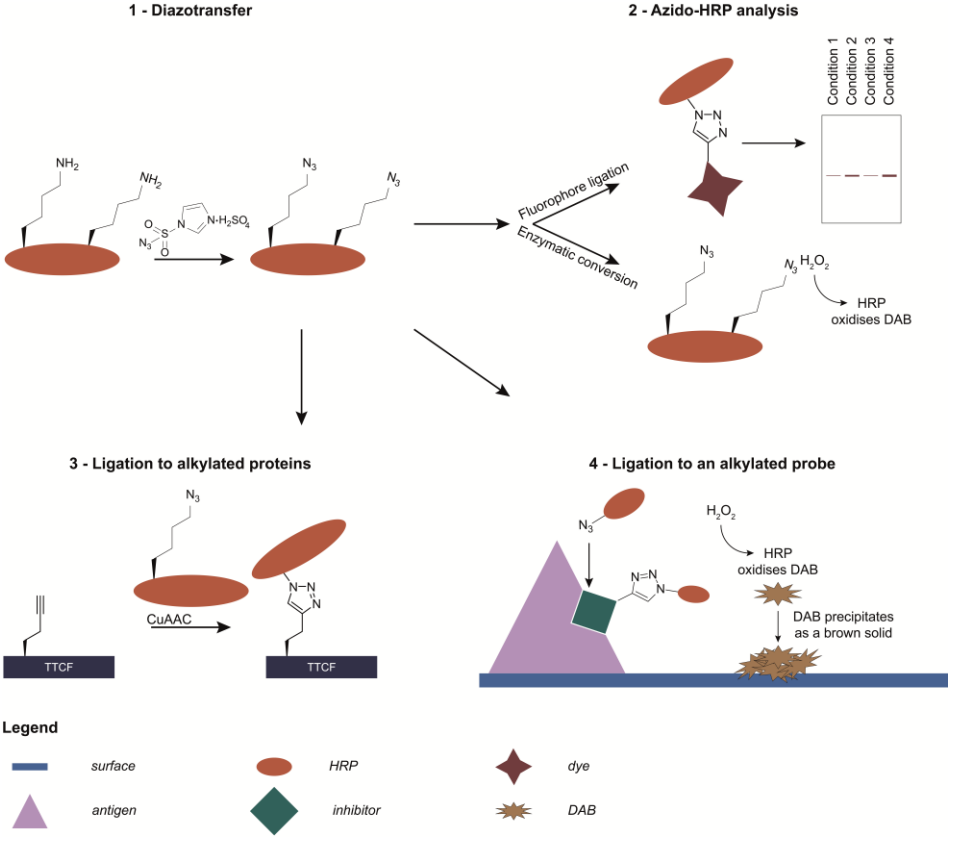

Figure 2. Schematic overview of the use of HRP-N_3. Different diazotransfer conditions to HRP were explored (**1**) and analyzed via e.g. fluorescent labeling or DAB precipitation studies (**2**). Next, the possibility to ligate this moiety to alkynylated proteins and bacteria were analyzed (**3**) and subsequently followed by testing its use in probe targeting studies (**4**).

biomolecule and a Staudinger ligation [39] or a Cu(I)-catalyzed azide-alkyne cycloaddition (CuAAC) [40] can be used to ligate a reporter molecule to the azide. In terms of histology, click chemistry, a fast ligation reaction between i.e. an alkyne and an azide [40], has been used to successfully image the bacterial peptidoglycan layer in sputum samples [41], but its use in histology has been relatively unexplored. The work in this Chapter describes research efforts to develop a click-histology workflow, which would expand the histology toolbox.

In 2007, Davis and co-workers described the production of azide/alkyne-containing β-galactosidase [42], which could serve as an enzyme in the click-histology workflow, as this histology-compatible enzyme remained active even after chemical

modification using ligation reactions. In 2009, Van Dongen *et al.* described the use of the diazotransfer reagent developed by Stick and co-workers [43] to azidylate the six lysine residues and the N-terminal amine of HRP without loss of peroxidase activity [44, 45]. It was thus postulated that these reagents could serve as histological tools for visualizing the presence of click handles. In this Chapter it was chosen to explore azido-HRP as a reagent, due to the tetrameric nature and more complex purification of β-Gal [42].

Results

The first steps in the exploration of azido-HRP as a histological click reagent was the optimization of the diazotransfer conditions to maximize the number of azide groups per protein without affecting its catalytic ability (Figure 2 - step 1). This was done in two steps. The efficiency of the diazotransfer reaction was assessed by qualifying their reactivity using a Cu(I)-catalyzed azide-alkyne cycloaddition (CuAAC) also known as Cu(I)-catalyzed Huisgen cycloaddition (ccHc) with a fluorescent (Alexa Fluor 647 (AF647)-conjugated) alkyne. The enzymatic activity of the HRP proteins that had undergone diazotransfer under various conditions was assessed by their ability to convert ABTS and DAB (Figure 2 - step 2). The azido-HRP constructs featuring optimal enzymatic activity is evaluated as click reagent in the second part of the Chapter (Figure 2 - step 3 and 4).

4.1 Optimization of the diazotransfer reaction

In first instance, the diazotransfer conditions as described by van Dongen *et al.* were evaluated [44]. In their original protocol, van Dongen *et al.* reacted 1 eq. of HRP with 13 eq. of imidazole-1-sulfonyl azide hydrogen sulfate (Stick's reagent) and 8.8 eq. of copper in 4.3 mM K_2CO_3 buffer. To see whether this reaction could be further optimized, the pH, Stick-reagent and copper concentrations were varied (Table 1). After purification over an Amicon Ultra spin column the efficiency of the reaction was determined by conjugation of an AF647 alkyne using CuAAC conditions.

In terms of the reactivity of HRP, van Dongen *et al.* modified on average four amines into azido residues [44]. In this study, the reaction could not be further

Table 1. Overview of the different diazotransfer conditions. The most optimal conditions as derived from the fluorescent ligation reaction and the initial ABTS analysis. The azidylated conditions used for further investigation (condition E, I, J and van Dongen HRP) are noted with an asterisk.

Reaction	HRP (eq.)	K_2CO_3 (conc. or eq.)	$Cu(II)SO_4.5H_2O$ (eq.)	Stick (H_2SO_4; eq.)	Fluorescent signal (%)	Activity (eq.)
A	1.0	100 mM, pH 8	1.1	20	38 ± 35	81
B	1.0	100 mM, pH 8	1.1	10	46 ± 4	103
C	1.0	100 mM, pH 8	1.1	5	28 ± 1	107
D	1.0	100 mM, pH 8	1.1	1	8 ± 1	109
E*	1.0	100 mM, pH 9	1.1	20	88 ± 15	154
F	1.0	100 mM, pH 9	1.1	10	79 ± 21	106
G	1.0	100 mM, pH 9	1.1	5	54 ± 6	99
H	1.0	100 mM, pH 9	1.1	1	13 ± 1	93
I*	1.0	100 mM, pH 10	1.1	20	129 ± 11	142
J*	1.0	100 mM, pH 10	1.1	10	98 ± 10	82
K	1.0	100 mM, pH 10	1.1	5	64 ± 10	103
L	1.0	100 mM, pH 10	1.1	1	12 ± 1	117
van Dongen HRP*	1.0	127.3	8.8	12.6	100 ± 0	100
HRP	1.0	-	-	-	0 ± 0	100

optimized: lowering the pH to 8 reduced the diazotransfer yield (conditions A-D; Table 1), as did lowering of the amount of Stick's reagent. The optimal ligation range was found to be pH 9-10 with 10-20 equivalents Stick's reagent (entries E, I, J; Table 1 and Figure 3A and B). The residual catalytic activity did not vary significantly between the different reaction conditions when assessed with an ABTS assay [44]. All of the azidylated proteins remained catalytically active with an observed activity ranging from 81 - 154% of that of the unmodified wild type counterpart (Table 1 and Figure 3C). Which means that the

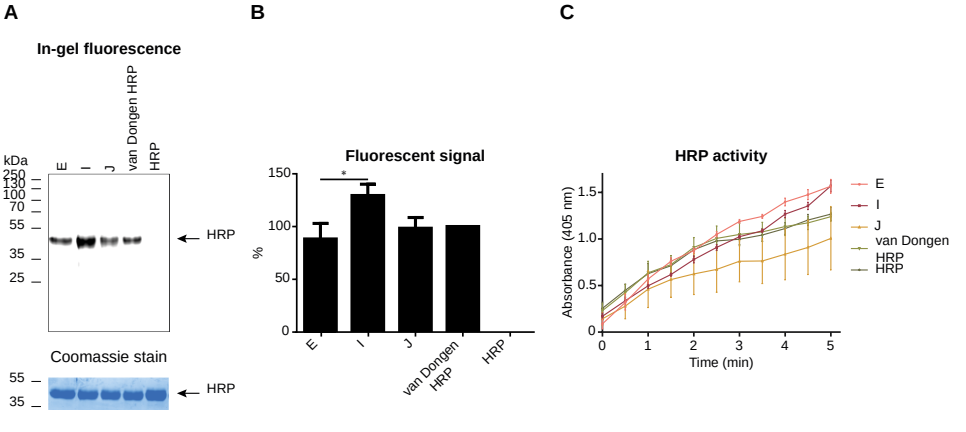

Figure 3. Analysis of the different azidylated HRP proteins compared to native HRP. A) Representative in-gel fluorescence after AF647 alkyne ligation to the differently derived azidylated HRP proteins (conditions E, I, J and van Dongen HRP). B) Intensity in % of the fluorescent signal compared to azido-HRP. C) Colorimetric conversion of ABTS by HRP and its azidylated versions with in Table 1 the corresponding activity as compared to unmodified HRP. Data is expressed as mean ± SD (N = 3, n = 1). Statistical analysis was performed using Tukey's multiple comparisons test. * $P \leq 0.05$.

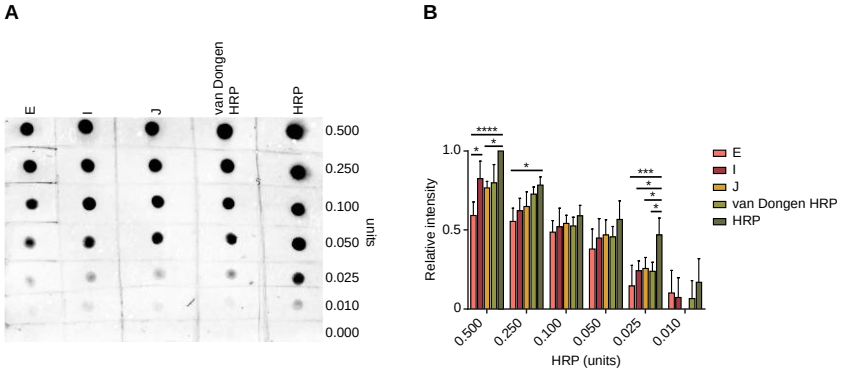

Figure 4. Dot blot analysis of various amounts of modified HRP and native HRP. The dots were dotted onto a PVDF membrane and visualized with commercially available DAB and imaged after 3-4 minutes of enzymatic reaction. A) Representative dot blot of the differently derived HRP proteins. This shows in B) the relative intensity of the dots, normalized to HRP 0.500 units. The activity of the azidylated proteins was in some cases significantly reduced, with condition I seen as most comparable to native HRP. Data represent means ± SD (N = 3, n = 1). Statistical analysis was performed using Tukey's multiple comparisons test. **** $P \leq 0.0001$; *** $P \leq 0.001$; * $P \leq 0.05$.

conditions as described by van Dongen *et al.* were near optimal for our purposes [44].

Azido-HRP produced by using conditions E, I and J, and the van Dongen conditions were next compared with wild type HRP, using a concentration range of the modified enzymes in a dot blot analysis. After blocking and washing, the membrane containing HRP-N_3 was incubated with DAB substrate and the amount of brown precipitate formed was assessed. Despite an absence in activity differences in the ABTS assay, here significant variance between the differentially produced HRP was observed (Figure 4A and B). The limit of detection of van Dongen, condition E, condition I and wild type was >0.010 units, whereas the limit of detection for condition J was >0.025 units. For all subsequent experiments, condition I (pH 10, 20 eq. Stick's Reagent) was used to produce HRP-N_3.

4.2 Ligation reactions

It was next tested whether HRP-N_3 could be used for the visualization of alkynylated proteins on membrane. For this, either alkynyl-TTCF (TTCF-Hpg; produced as described in more detail in **Chapter 2** and **3** [46, 47]), containing eight homopropargylglycine (Hpg) residues per protein (including the start codon), or wild

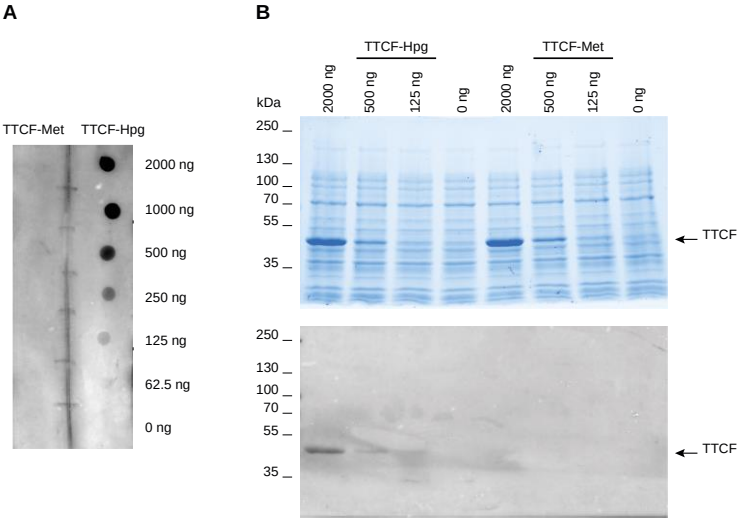

Figure 5. HRP-N_3 ligation to folded and unfolded TTCF-Hpg. A) The TTCF-Hpg and TTCF-Met proteins were dotted in a non-denatured state on a PVDF membrane, and after CuAAC reaction with HRP-N_3 as reporter molecule, HRP was visualized with DAB precipitation. This resulted in visualization of only TTCF-Hpg as low as 62.5 ng of protein. B) TTCF-Hpg and TTCF-Met were combined with B834 cell lysate in different concentrations and run over a 10% TGX Stain-Free gel. After visualization of the proteins in a Stain-Free gel (upper panel), the gel was transferred to a PVDF membrane and a CuAAC reaction was performed on blot with HRP-N_3 as ligating molecule. HRP was visualized with DAB precipitation (lower panel). The resulting precipitate was only visible at positions where TTCF-Hpg was present (2000, 500 and 125 ng of protein).

type TTCF was serially diluted and dotted onto a polyvinylidene difluoride (PVDF) membrane followed by a blocking step with 5% nonfat dry milk. The membrane was then subjected to a CuAAC ligation mixture, containing 13 µM azido-HRP in presence of 3 mM copper sulfate, 30 mM sodium ascorbate, 3 mM THPTA ligand, 30 mM aminoguanidine-HCl in 88 mM HEPES pH 7.2. The copper ions of the ligation reaction were removed to prevent interference with the DAB oxidation, by washing with 100 mM EDTA [20, 48]. Next, the blots were subjected to DAB-staining, which resulted in visible DAB precipitation for the serially-diluted TTCF-Hpg (limit of detection 62.5 ng/1.2 pmol protein; Figure 5A). No signal was observed at any concentration in the negative control (use of native TTCF). This experiment showed the possibility to ligate HRP-N_3 to a non-denatured protein and to visualize this via DAB precipitation.

Next, the specificity of the CuAAC ligation reaction was assessed by serially diluting the TTCF-Hpg and TTCF-Met in *Escherichia coli* (*E. coli*) lysate. The resulting mixtures

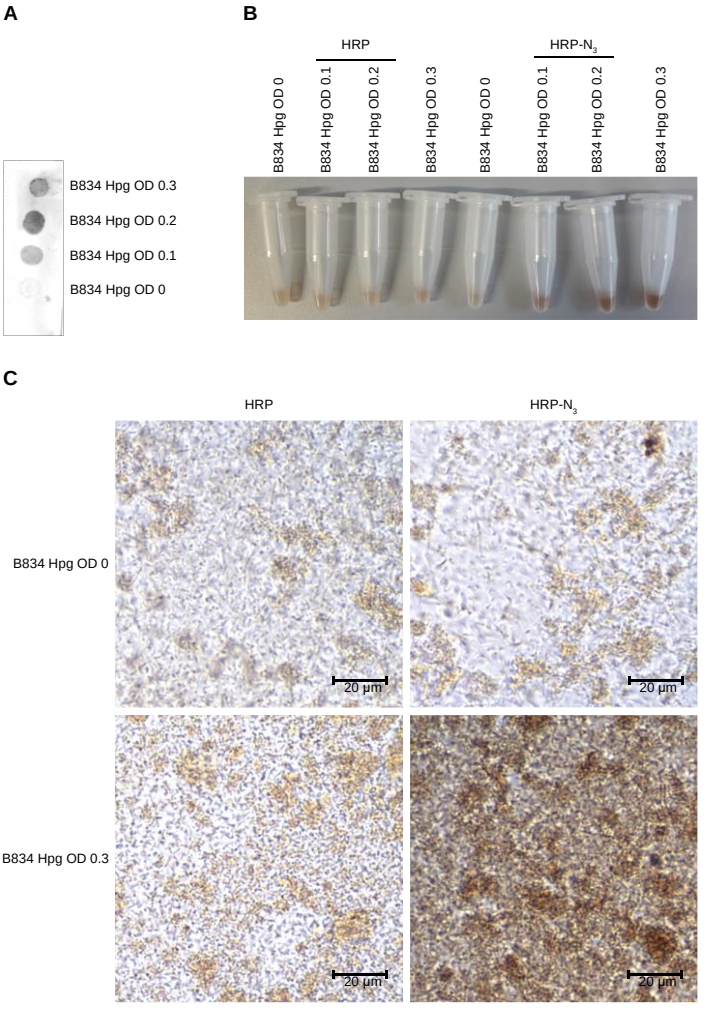

Figure 6. HRP-N_3 ligation to alkynylated bacteria, enzymatically reacted with DAB. A) Representative blot of a serial dilution of alkynylated bacteria, ligated to HRP-N_3. Which showed an increase in DAB precipitation with an increased concentration of alkynylated bacteria. The dot blot was representative for the performed triplicate. B) Visualization of the DAB precipitation performed in solution phase after ligation to HRP and HRP-N_3 and C) the microscopic analysis of the ligation reaction. The DAB signal of the alkynylated bacteria reacted with HRP-N_3 was higher than background.

were separated in a TGX Stain-Free gel and transferred to a PVDF-membrane. The resulting blot was reacted with 40 eq. of HRP-N_3, followed by washing with buffer containing imidazole [49], citric acid [50] and EDTA [51], again to remove residual copper ions. Reaction with DAB yielded a detectable signal at the expected protein size of 53 kDa, with a detection limit of 125 ng (2.3 pmol, corresponding to 18.7 pmol of

alkyne moieties; Figure 5B, lower panel). Furthermore, the blot and the accompanying gel confirmed the selectivity of the ligation reaction (Figure 5B).

4.3 Bacterial cell labelling

After establishing that HRP-N_3 can be used to visualize alkynylated proteins, it was next explored whether this approach could also be used to detect alkynes in a model immunocytochemical setting. This setting was simulated on dot blot and in a solution phase experiment, using *E. coli* bacteria of which one population was labeled with L-Hpg and the other one was unlabeled. For this, the *E. coli* methionine auxotroph B834 was used and either grown to exponential phase in LB medium or in the presence of L-Hpg for metabolic labelling [46]. After growth, the mixtures of alkynylated and unmodified bacteria were washed, fixed with 4% PFA, permeabilized with either 0.1% IGEPAL or 0.15% Triton X-100, washed and subsequently incubated with 1% H_2O_2 to block endogenous peroxidases [52, 53]. After an additional washing step, the mixtures were dotted onto PVDF membrane, blocked with 5% milk and subjected to a CuAAC ligation mixture. Subsequently, the membrane was washed as before and stained with DAB. Imaging the blots showed the DAB precipitation to be dependent on the percentage Hpg-labeled *E. coli* present in each sample. (Figure 6A). Similar results were obtained when the reaction was performed in liquid phase (Figure 6B and C). These experiments showed that the approach is compatible with a histological workflow.

4.4 In-cell labelling of an enzyme activity

One of the main areas where bioorthogonal reactions are truly additive to antibody stainings is in the in-cell detection of enzyme activities [54, 55]. By introducing ligation handles into covalent enzyme inhibitors, active populations of a particular enzyme can be visualized (Figure 2 - step 4); something that is not possible using antibody techniques. In this manner, cathepsins [56], post-proline proteases [57], cysteine proteases [58, 59] and serine proteases [60, 61] have been visualized, to name but a few. The approach is also moving to the clinic for e.g. the identification of tumor boundaries [62]. As conventional tumor histology is done using immunohistochemical approaches,

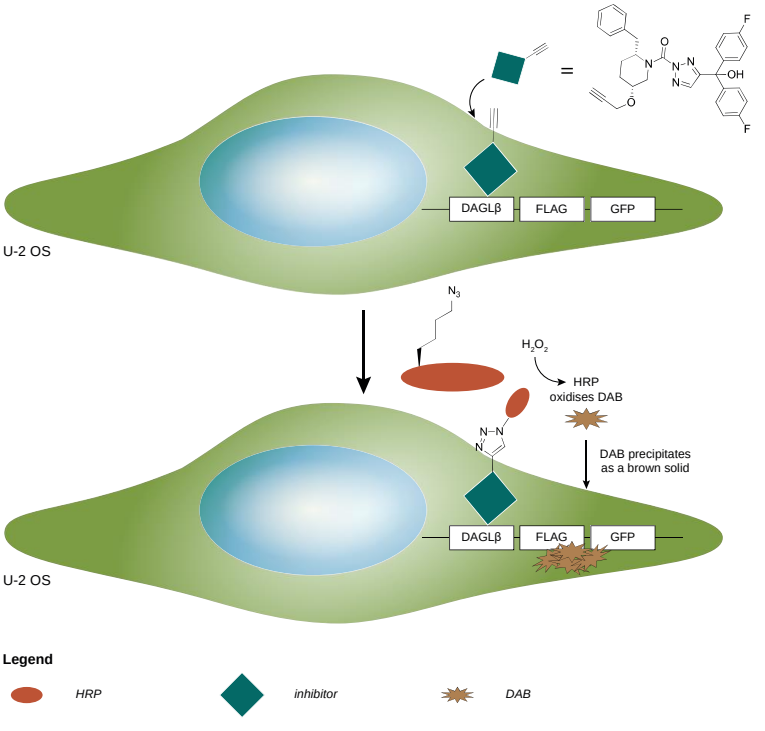

Figure 7. Schematic overview of HRP-N_3 ligation to probe DH376 which can inhibit i.e. DAGLβ. This overview shows the inhibition of DAGLβ by DH376 (left) and the ligation of HRP-N_3 with a CuAAC reaction. When reacting with DAB, precipitation should occur only at the site of the protein inhibited by the alkyne containing probe.

it was attempted to combine activity-based protein profiling (ABPP) and CuAAC ligation with HRP-N_3 staining.

Two stable U-2 OS cell lines expressing the serine hydrolases DAGLβ (unpublished) and ABHD6 [63] combined with a FLAG-tag, for immunoblotting, and a GFP reporter gene, for fluorescent colocalization, were used to demonstrate this concept. The two serine hydrolases were labeled with an alkyne-containing inhibitor of the enzymes, DH376 (Figure 7) [64].

At first, it was tested what the limit of detection was for detecting an ABP-labeled enzyme with HRP-N_3 by Western blot using luminol as substrate for the DAGLβ-FLAG-GFP cell construct. The protein was reacted with 100 nM of the alkyne-containing ABP DH376 *in situ* and the cell lysate resolved in a TGX Stain-Free gel, prior to being transferred to a PVDF membrane. Western blot analysis was performed using antibodies

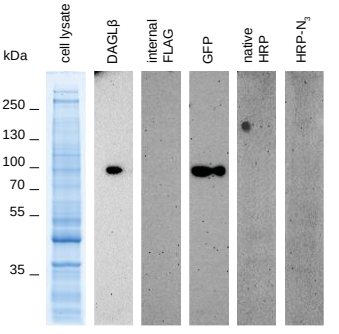

Figure 8. Western blot analysis of the construct and HRP-N_3 ligation to probe DH376. Cell lysate and Western blot analysis of a DAGLβ-FLAG-GFP cell line treated with DH376. Western blot was performed against DAGLβ, FLAG and GFP. The PVDF membrane containing the cell lysate was furthermore reacted with HRP and HRP-N_3 in the presence of a CuAAC ligation mixture. HRP-N_3 could not be visualized using a chemiluminescent readout.

against DAGLβ, FLAG and GFP. Alternatively, the blots were exposed to a CuAAC ligation mixture containing either HRP or HRP-N_3. These experiments show that the protein could readily be visualized by Western blot (using a chemiluminescent readout) against DAGLβ (~100 kDa protein (DAGLβ is a 74 kDa and GFP a 27 kDa protein) and GFP (Figure 8, panel "DAGLβ" and "GFP"), but not the FLAG-tag (Figure 8, panel "internal FLAG"). Moreover, the ligation reaction with HRP(-N_3), failed to yield a detectable signal (Figure 8, panel "native HRP" and "HRP-N_3").

The detection was also attempted in whole cells using microscopy and DAB-precipitation. For this, cells containing either the DAGLβ or ABHD6 construct were treated with 100 nM DH376 and fixed with 4% paraformaldehyde (PFA). These cells were permeabilized with 0.15% Triton-X100 and a CuAAC ligation reaction was performed in the presence of HRP-N_3 or HRP (as negative control). After washing the cells with a 100 mM EDTA wash buffer and PBS, the cells were subjected to DAB precipitation and subsequently washed with PBS. Microscopic analysis of the cells showed that no DAB precipitation could be observed that correlated with enzyme presence for DAGLβ and only marginally for ABHD6 (Figure 9). The presence of DAB precipitate led to a decrease in GFP signal [65, 66].

It was therefore hypothesized that either the alkyne handle of DH376 was buried in the active site of the enzyme, or the fixation and/or permeabilization of the cells was

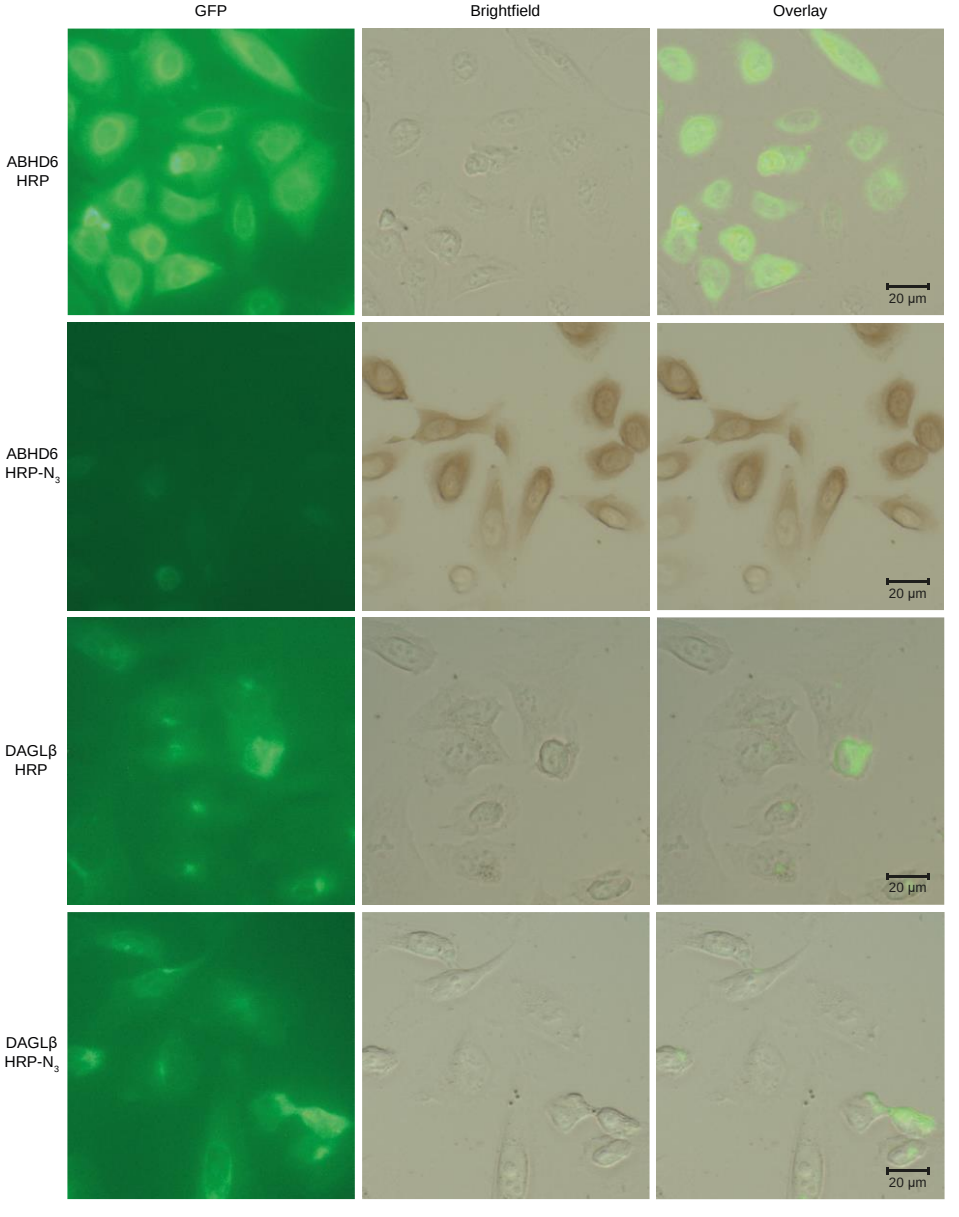

Figure 9. Microscopic analysis of DAB precipitation after probe treatment of DAGLβ-FLAG-GFP containing cells. Both the GFP signal, the brightfield signal and an overlay of these two signals were displayed. DAB precipitation is visible on cells treated with HRP-N_3, but not in cells reacted with HRP. None of the treated cells showed a GFP signal.

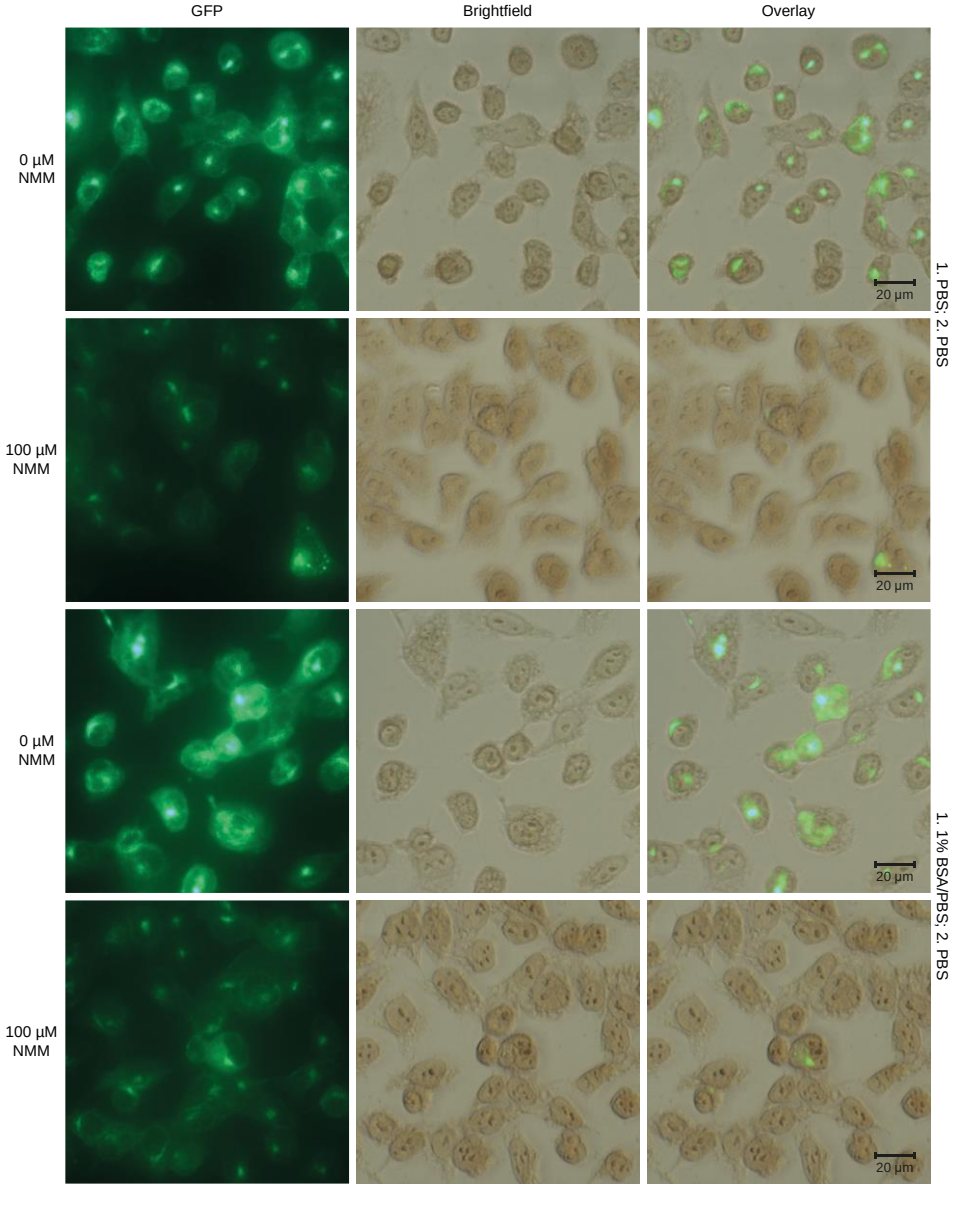
GFP
Brightfield
Overlay
0 µM NMM
100 µM NMM
0 µM NMM
100 µM NMM
20 µm
20 µm
20 µm
20 µm
1. PBS; 2. PBS
1. 1% BSA/PBS; 2. PBS

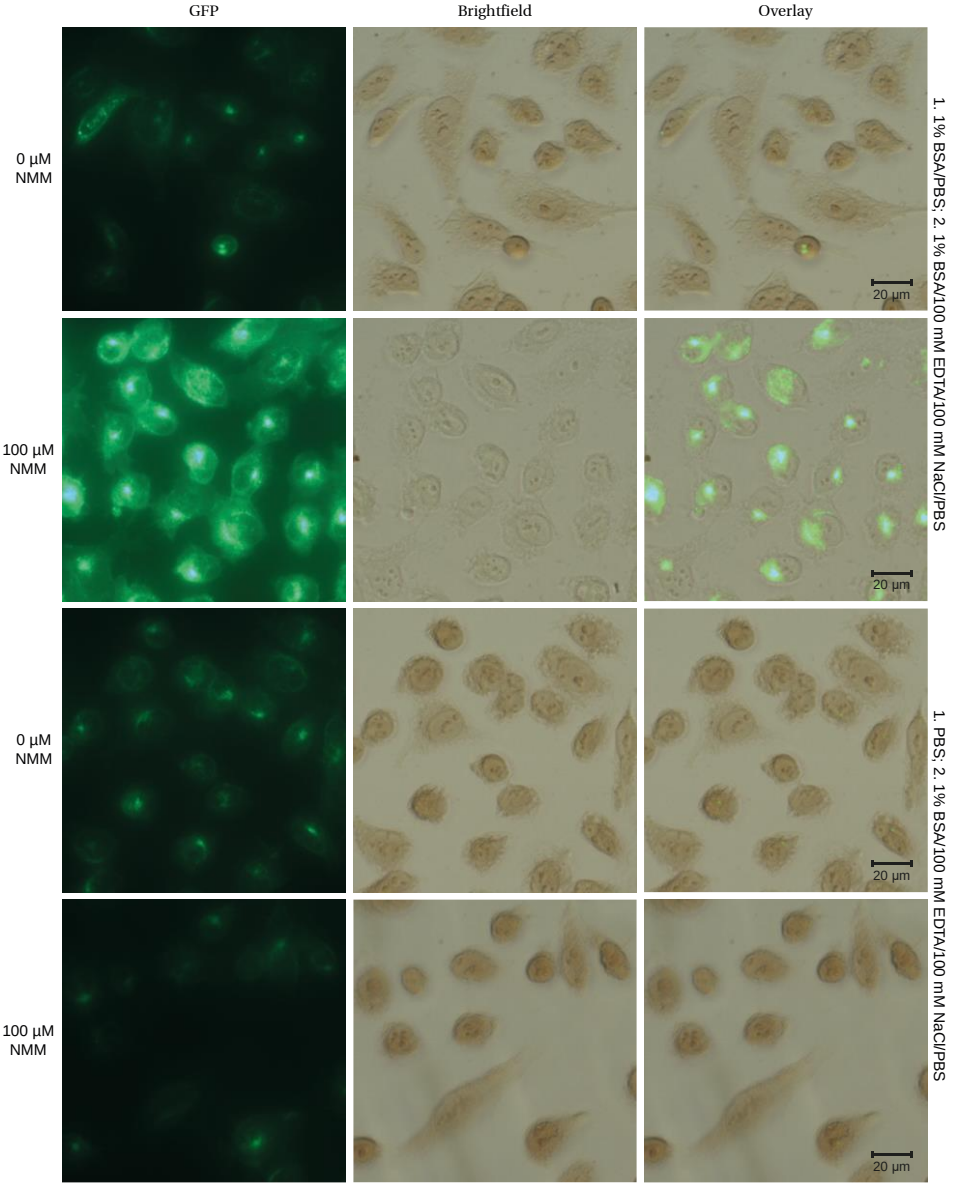

Figure 10. The use of different blocking agents. Different wash steps were combined with and without blocking the free amines with NMM. Wash step 1, with either PBS or 1% BSA/PBS, was performed before the addition of HRP and wash step 2, with either PBS or 1% BSA/100 mM EDTA/100 mM NaCl/PBS was performed after the addition of HRP.

unsuccessful. The fixation and permeabilization steps were varied in order to obtain increased DAB precipitation. Cells were treated with the following different

fixative/permeabilizer agents: acetone, methanol, methanol:acetone 1:1 and methanol:ethanol 1:1. Moreover, PFA fixation was combined with permeabilization by digitonin and saponin. These conditions resulted in the formation of brown precipitate for both the HRP-N_3 ligation and the negative control (HRP).

The formation of brown precipitate in the negative control was hypothesized to stem from aspecific binding and therewith an issue with incomplete blocking. Different blocking agents were therefore also assessed. First, immediately after methanol fixation the cells were washed with a mix of glycine/PBS (blocks free aldehydes) [67] and after blocking potential internal peroxidases with H_2O_2, free amines were blocked with N-methylmorpholine (NMM) buffered in PBS [68]. Furthermore, a combination of wash steps with BSA/PBS and BSA/EDTA/NaCl/PBS was introduced, the first before and the latter after the addition of HRP. The only blocking method that prevented cells to be stained brown was blocking with both 1% BSA/PBS and 1% BSA/100 mM EDTA/100 mM NaCl/PBS (Figure 10).

Some of the alternative wash steps showed samples free of background. This combination, 1% BSA/PBS and 1% BSA/100 mM EDTA/100 mM NaCl/PBS, was therefore used in a follow up experiment, using either HRP or HRP-N_3 in the ligation mix. Unfortunately, the DAB precipitation was higher in the negative control samples as compared to the samples (Figure 11), leading to the conclusion that this method is not sensitive enough for detecting the ABP.

Discussion and conclusion

This Chapter describes a new method for the visualization of alkynylated proteins and bacteria in immunohistological settings. In the first part of this Chapter the optimization of HRP-azidylation was attempted. The best condition – after analysis in a fluorescent and DAB precipitation assay – was found to be condition I (pH 10, 20 eq. Stick's Reagent). This means at higher pH and higher equivalents of Stick's Reagent, the diazotransfer to HRP resulted in the best azidylation with respect to its ligation and residual DAB activity.

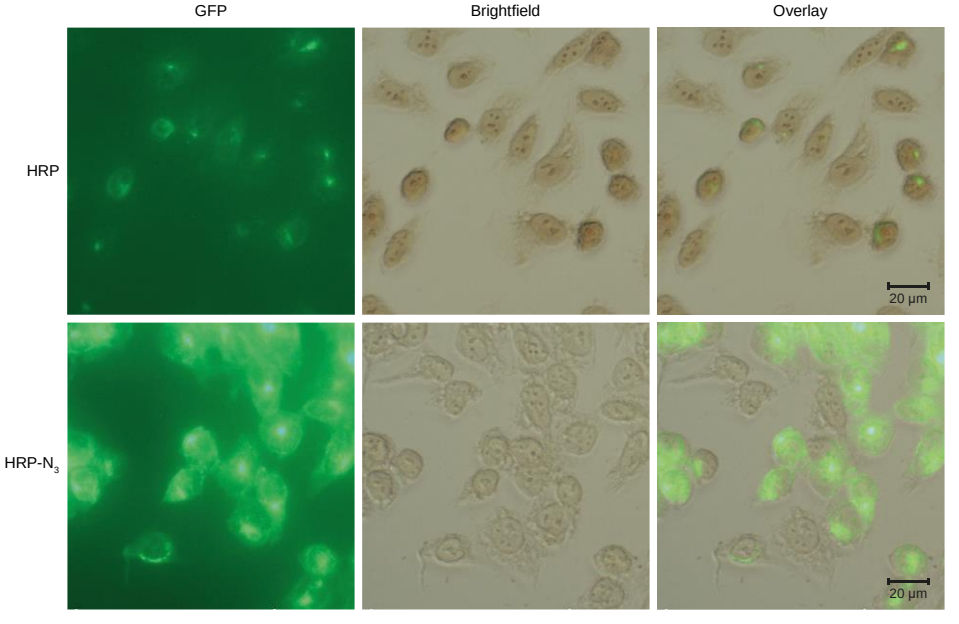

Figure 11. The use of NMM with blocking agents 1% BSA/PBS and 1% BSA/100 mM EDTA/100 mM NaCl/PBS. Upper panels: Background signal using HRP in the ligation mixture. Lower panels: The ligation reaction performed using HRP-N_3 in the ligation mixture.

This reagent was next used to detect the presence of alkyne groups in a variety of samples. For instance, the approach could be used to selectively detect an alkynylated protein in cell lysate, and the presence of labelled bacteria in a mixed population. It could not, however, be used to identify an alkyne-modified activity based probe in mammalian cell samples.

When working on the ligation of the bacterial cell lysates, it was shown that each of the experiments showed background staining with DAB. In each of them, 1% H_2O_2 was used to block endogenous peroxidases. However, literature data is available that this might not be the optimal condition for peroxidase blockade [49]. In future, it is suggested to repeat the ABTS reactivity experiment as described for alkynylated bacteria, using a concentration range of H_2O_2 with the aim to increase the signal-to-noise in the microscopic analysis which was described in the in cell labeling section of this Chapter.

The experiments in mammalian cells were less successful. The reaction of azido-HRP with an alkyne containing active site probe did not yield a detectable signal, either in a blot-experiment or in cell-based imaging assays. For now, it can be concluded that

azido-HRP is a useful tool for the detection of abundant loci of alkynes in samples, but not for approaches where few and/or diffuse labels are present.

Acknowledgements

Ward Doelman is kindly thanked for synthesizing THPTA, and Thomas Bakkum for synthesizing L-Hpg.

Materials and methods

General

All chemicals and reagents were purchased at Sigma-Aldrich, Alfa Aesar, Acros, Merck or VWR, unless stated otherwise. Reagents were used without further purification. Sodium dodecyl sulfate-polyacrylamide gel electrophoresis (SDS-PAGE), Stain-Free gel and Western blot materials were purchased at Bio-Rad. DH376 was previously synthesized in-house and characterized by NMR and LC-MS [64]. Cell culture disposables were from Sarstedt.

Solutions

PBS contained 5 mM KH_2PO_4, 15 mM Na_2HPO_4, 150 mM NaCl, pH 7.4 and PBST was PBS supplemented with 0.05% Tween-20. TBS contained 50 mM Tris-HCl, 150 mM NaCl and TBST was TBS supplemented with 0.05% Tween-20. Laemmli sample buffer 4* contained 60 mM Tris-HCl pH 6.8, 2% (w/v) SDS, 10% (v/v) glycerol, 5% (v/v) β-mercaptoethanol, 0.01% (v/v) bromophenol blue.

Compound synthesis

Imidazole-1-sulfonyl azide hydrogen sulfate

As described by Potter *et al.* [45]. A 250 ml round-bottomed flask with a stirring bar was brought under nitrogen atmosphere and cooled to 0˚C. Sodium azide (5.2 g, 80 mmol, 1.0 eq.) was added before the addition of dry EtOAc (80 mL). After adding SO_2Cl_2 (6.5 ml, 80 mmol, 1.0 eq.) over 10 min the reaction was slowly warmed to rt and left stirring under an inert atmosphere overnight. The reaction mixture was then recooled to 0˚C, before the addition of imidazole (10.9 g, 160 mmol, 2.0 eq.) and the resulting suspension was stirred for 3.5 h at 0˚C. The reaction mixture was basified with saturated aqueous $NaHCO_3$ (150 mL). The organic layer was separated from the aqueous layer, washed with H_2O and dried with $MgSO_4$. The suspension was filtered and cooled to 0˚C. Concentrated H_2SO_4 (4.4 ml, 80 mmol, 1.0 eq.) was added over 5 min. The mixture was warmed to rt and stirred until a precipitate had formed, which was filtered and washed with EtOAc. The remaining white crystals were dried under vacuum to afford the title compound pure (12.8 g, 47 mmol, 59%).

Synthesis of tris-hydroxypropyltriazolylmethylamine (THPTA)

A two-step synthesis as described before by Hong *et al.* [70].

Synthesis of (S)-2-Aminohex-5-ynoic acid (L-Hpg)

Synthesis as described before by Li *et al.* [71], followed by a procedure based on Biagini *et al.* [71], Dong *et al.* [72] Chenault *et al.* [73] to obtain the chirally pure variant.

HRP modification and analysis

Diazo-transfer to HRP

Adjusted from van Dongen *et al.* (2009) [44]. To a solution of HRP (263-325 units/mg; P8375 10kU) in MQ (2.5 mg/mL) an aqueous solution of K_2CO_3 (either 2 mg/mL or 100 mM, pH 8-10) was added. Subsequently followed by the addition of $CuSO_4.5H_2O$ (1 mg/mL) and Stick's reagent (2 mg/mL) and the reaction was left shaking at 20˚C 500 rpm overnight. The mixture was transferred to an Amicon Ultra spin filter with either a 3 or 10 kDa cutoff and centrifuged to dryness. The protein was redissolved in MQ water and centrifuged for another 5-8 washings. The end product was redissolved in MQ water and the presence of click handles was visualized via fluorescence analysis. Bradford analysis, with BSA as standard, was used to measure protein concentrations.

Fluorescent analysis of HRP-N_3

HRP-N_3 was characterized by ligating Alexa Fluor 647 (AF647) alkyne to the azide click handle. This was done via CuAAC reaction, protein was combined 2:1 (v/v) with click mix (containing 3 mM copper sulfate, 30 mM sodium ascorbate, 3 mM THPTA ligand, 30 mM aminoguanidine-HCl and 14 µM AF647-alkyne in 88 mM HEPES pH 7.2, final concentration in click mix) reaction for 1 hour at rt in the dark. The reaction was quenched by the addition of 4* Laemmli buffer. Samples were resolved in a 10% SDS-PAGE gel (180 V, 75 min) along with PageRuler™ Plus Protein Marker (Thermo Scientific), before scanning Cy3 and Cy5 multichannel settings (605/50 and 695/55 filters, respectively; ChemiDoc™ MP System, Bio-Rad). Coomassie staining (Coomassie Brilliant Blue R-250) was used for correcting protein loading and quantification was done using Image Lab (Bio-Rad).

Activity assay

Adjusted from Van Dongen *et al.* [44]. All solutions were kept on ice until measurement. A solution of ABTS/H_2O_2 (8 mM ABTS in 20 mM sodium phosphate buffer, pH 7.4 containing 0.2% H_2O_2) was prepared fresh before each measurement. HRP or HRP-N_3 was diluted to 2.5 units/mL in 20 mM sodium phosphate buffer, pH 7.4 and fractionate 100 µL per well of a 96 well plate. As a control 100 µL of phosphate buffer was used. To each well, 5 µL of ABTS/H_2O_2 solution was added immediately before measuring the absorption at 405 nm on a TECAN Infinite M1000 Pro plate reader.

Bacterial growth and protein expression

B834 growth

B834 was inoculated in triplicate with 1:100 diluted ON culture grown in LB medium. The cells were grown until an OD_{600} of ~0.8 and sedimented in aliquots to a final OD_{600} of 0.2 and stored until use at -20˚C.

Expression and purification of recombinant TTCF

Adjusted from Antoniou *et al.* (2000) [75]**.** An overnight culture of B834 containing pET16b_TTCF (earlier cloned from the pEH101 plasmid, kindly provided by prof. C. Watts) was diluted 1:100 in LB medium containing 50 µg/mL ampicillin and 1% glucose. Cells were grown at 37˚C, 180 rpm to an OD_{600} of ~0.8 and sedimented (3428 rcf, 15 min, 4˚C) before being washed twice with SelenoMet medium (Molecular Dimensions). Cells were resuspended in SelenoMet medium containing 50 µg/mL ampicillin and depleted for 30 min at 37˚C, 180 rpm before 30 min depletion at 30˚C, 130 rpm. After this either L-Methionine (L-Met; 40 mg/L; Ajinomoto) or L-Homopropargylglycine (L-Hpg; 40 mg/L) was added to the culture and 15 min later the culture was induced with isopropyl-β-D-thiogalactopyranoside (IPTG; 1 mM final concentration) and expression took place ON. After overnight expression, cells were pelleted and washed once with PBS. Pellets were stored at -80˚C until protein purification. A 1 L culture pellet was resuspended in 15 mL lysis buffer containing 100 mM Tris-HCl pH 8.0, 500 mM NaCl, 10 mM imidazole, 10% glycerol, 1 mg/mL lysozyme, 250 U benzonase. Lysis took place for 20 min at rt, before separating the soluble from the insoluble protein (10000 rcf, 15 min, 4˚C). The supernatant was filtered over a 0.2 µm filter and loaded on a 5 mL His-column (Ni-NTA

Superflow Cartridge; Qiagen). After loading, the column was washed with 5 CV of IMAC25 buffer (100 mM Tris-HCl pH 8.0, 500 mM NaCl, 25 mM imidazole), before eluting with a 15 CV gradient 25 - 500 mM imidazole. The protein fractions were monitored by SDS-PAGE as described before and Coomassie staining revealed the purity of the protein. The fractions containing the most pure protein were combined and extensively dialysed (6 - 8 kDa MWCO, 3.3 mL/cm, FisherBrand or 12 - 14 kDa MWCO, 2 mL/cm, Spectra/Por) against PBS. The protein was concentrated over an Amicon spin filter 10 kDa MWCO, before being aliquoted, flash frozen and stored at -80˚C until further use.

Dot blot and Western blot analysis

HRP and HRP-N_3

A serial dilution of HRP and HRP-N_3 was made and 2 µL was pipetted onto a PVDF membrane to form a dot. The protein was spotted on three separate membranes, dried for 1 h and blocked in 5% nonfat dry milk (Elk; Campina) in TBST at room temperature for 1.5 h or at 4˚C ON. Subsequently washed 3x with TBST and 1x with TBS before adding DAB substrate (BD Biosciences). After 3-4 minutes the membranes were imaged on a ChemiDoc™ MP System, Bio-Rad and quantified by ImageJ.

Recombinant protein

A serial dilution of TTCF-Hpg was made and 2 µL was pipetted onto PVDF membrane to form a dot. The protein was spotted on three separate membranes, dried for 1 h and blocked in 5% nonfat dry milk (Elk; Campina) in TBST for 1.5 h at room temperature. HRP-N_3 was ligated to the proteins as described for fluorescence analysis, using 12.8 µM (349 eq. N_3 - alkyne) HRP-N_3 instead of a fluorophore. The blot was washed 3x with 100 mM EDTA in TBST, 3x with TBST and 1x with TBS. Subsequently DAB was added and after 3-5 minutes the membranes were imaged on a ChemiDoc™ MP System, Bio-Rad and quantified by ImageJ.

Western blot analysis

Samples were resolved in a 10% Stain-Free gel (proteins at indicated concentrations or 20 µg cell lysate) along with PageRuler™ Plus Protein Marker (Thermo

Scientific) and transferred onto a PVDF membrane by Trans-Blot Turbo™ Transfer system directly after scanning. Membranes were washed with TBS and TBST and blocked with 5% nonfat dry milk (Elk; Campina) in TBST at rt for 1.5 h or at 4˚C ON.

Membranes containing cell lysates were then incubated with primary antibody in 5% nonfat dry milk (Elk; Campina) in TBST (GFP; FLAG; 1 h at rt) or washed 3x times with TBST and incubated with DAGLβ in 5% BSA in TBST (4˚C, ON). Membranes were washed 3x with TBST and incubated with matching secondary antibody in 5% nonfat dry milk (Elk; Campina) (1 h at rt). Subsequently washed three times with TBST and once with TBS. Membranes were developed with luminol (10 mL of 1.4 mM luminol in 100 mM Tris, pH 8.8 + 100 µL of 6.7 mM p-coumaric acid in DMSO + 3 µL of 30% (v/v) H_2O_2) [76] and chemiluminescence was detected on the ChemiDoc™ MP System in the chemiluminescence channel and protein marker was visualized with Cy3 and Cy5 settings (605/50 and 695/55 filters, respectively).

Membranes used for HRP-N_3 ligation were washed 3x times with TBST and a ligation mixture containing HRP or HRP-N_3 (42 eq. or 0.86 nmol) was added (1 h at rt). Subsequently washed 3x with 10% (w/v) citric acid, 100 mM EDTA, pH 8.0, 500 mM imidazole, 3x with TBST and 1x with TBS. Before detecting with DAB substrate or chemiluminescence as described before.

Primary antibodies: monoclonal mouse anti-FLAG M2 (1:5000, Sigma Aldrich, F3156), monoclonal anti-GFP (1:2500, Thermo-Fisher, GF28R), Monoclonal anti-DAG Lipase β (1:1000, Cell Signaling, D4P7C)

Secondary antibodies: mouse IgG_K BP-HRP (1:5000, Santa Cruz, sc-516102), mouse anti-rabbit IgG-HRP (1:5000, Santa Cruz, sc-2357).

Analysis of alkynylated bacteria

B834 growth and storage

B834 was inoculated in triplicate with 1:100 diluted ON culture grown in LB medium. The cells were grown until an OD_{600} of ~0.7-0.8 and sedimented before being resuspend in SelenoMet medium containing either L-Met or L-Hpg. Cells were grown for another 2 hours, before an OD of 0.5 was sedimented. Cells were resuspended in 1 mL of 4% PFA and fixed for 20 min at rt. Fixed cells were washed once with PBS and stored at an OD_{600} of 0.4 in PBS at 4˚C.

DAB visualization

Bacterial cells were combined to reach the wanted OD of alkynylated bacteria and solubilized with either 0.1% IGEPAL or 0.15% Triton X-100 for 20-25 min at rt, before being washed once with PBS. Afterwards cells were incubated with 1% H_2O_2 to block endogenous peroxidases. Washed once more with PBS and resuspended in a CuAAC ligation mixture (containing 3 mM copper sulfate, 30 mM sodium ascorbate, 3 mM THPTA ligand, 30 mM aminoguanidine-HCl and 1 nmol HRP(-N_3) in 88 mM HEPES pH 7.2, final concentration in click mix) for 1 h at rt in the dark. After ligation, cells were washed 3x with 100 mM EDTA and 1x with PBS. Pellet was resuspended in DAB substrate and visualized by visible imaging and microscopic analysis (EVOS FL Auto 2).

Or as described for *recombinant protein,* with minor adjustments.

Cell culture

General cell culture

Cell lines were purchased at ATCC and tested on regular basis for mycoplasma contamination. Cultures were discarded after 2-3 months of use. U-2 OS cell lines expressing either ABHD6 or DAGLβ were kindly provided by A.C.M. van Esbroeck and cultured at 37˚C under 7% CO_2 in DMEM containing phenol red, stable glutamine, newborn bovine serum (10% v/v; Seradigm), G418 (400 µg/mL; supplier) penicillin (200 IU/mL; Duchefa) and streptomycin (200 µg/mL; Duchefa). Medium was refreshed every 2-3 days and cells were passaged two times a week at 80-90% confluence.

ABHD6/DAGLβ inhibition by DH376

U-2 OS cells were seeded at appropriate density one day before treatment (1:250 - 1:400 for 8-well chamber slides (Ibitreat; Ibidi) and 1:10 - 1:15 in culture dishes for the preparation of cell lysates). Culture medium was removed and treatment medium, containing 100 nM DH376, was added.

Cells were trypsinized after incubation for 1 h at 37˚C and 7% CO_2, washed 1x with PBS and spun down (3000 rcf, 5 min, rt). Cell pellets were flash frozen and stored at -80˚C until further use.

For microscopic analysis, medium was aspirated and cells were washed 2x with PBS following the experimental procedure as described below.

Microscopic analysis of treated U-2 OS cells

Cells used for different permeabilization methods were either fixed with 4% PFA in PBS (15 min, rt), washed 1x with PBS and permeabilized with 0.15% Triton X-100, 100 µM Digitonin or 0.5% Saponin in PBS or in one step fixed and permeabilized with solvents acetone, methanol, 1:1 (v/v) methanol:acetone or 1:1 (v/v) methanol:ethanol for 10 min at -20˚C and washed 2x with PBS. Subsequently washed 2 or 3x with PBS(T) and 1% H_2O_2 in PBS (10 min, rt). A 2x wash with PBS(T) was performed before adding 10 µM (1.4 - 2 nmol) HRP(-N_3) 10 min prior to the click mix (containing 3 mM copper sulfate, 30 mM sodium ascorbate, 3 mM THPTA ligand and 30 mM aminoguanidine-HCl in 88 mM HEPES pH 7.2, final concentration in the mix) or in the click mix itself. After 1 hour, cells were washed 3x with 100 mM EDTA in PBS and 3x with PBS(T), before the addition of DAB substrate (15 min, rt) and cells were subsequently washed 2x with PBS and stored at 4˚C until microscopic analysis (EVOS FL Auto 2).

Cells used for wash optimization methods were fixed and permeabilized with ice-cold methanol for 10 min at rt. Before washing 3x with 100 mM glycine in PBS and 1x with 1% H_2O_2 in PBS (10 min, rt). Cells were washed 2x with PBS and blocked with 0 or 100 µM NMM in PBS (10 min, rt) and washed 1x with PBS. Followed by incubation with 1% BSA in PBS or PBS (20 min, rt) and washed 1x with PBS. HRP(-N_3) (1 nmol; 10 µM) was added and after 10 min, when necessary, a click mix (containing 3 mM copper sulfate, 30 mM sodium ascorbate, 3 mM THPTA ligand and 30 mM aminoguanidine-HCl in 88 mM HEPES pH 7.2, final concentration in the mix) was added and left for 1 h at rt. And added after ligation, or after 10 min HRP incubation, followed by 3x washing with 1% BSA/100 mM EDTA/100 mM NaCl in PBS or PBS and 3x PBS. DAB substrate was added to the chambers for 5 min, rt and cells were subsequently washed 2x with PBS and stored in PBS at 4˚C until microscopic analysis.

Preparation of cell lysates

Cell pellets were thawed on ice and resuspended in lysis buffer (250 mM sucrose, 20 mM HEPES pH 7.2, 1 mM $MgCl_2$, 2 mM DTT, 50 U/mL benzonase). Protein concentrations were determined using Quick Start™ Bradford Protein Assay (Bio-Rad) and diluted to convenient concentration in lysis buffer.

Statistical analysis

Replicates shown represent biological replicates and data represent means ± SD. All statistical analysis was determined using GraphPad Prism® 7/8 or Microsoft Excel 2016. **** $P \leq 0.0001$; *** $P \leq 0.001$; ** $P \leq 0.01$; * $P \leq 0.05$; NS if $P > 0.05$. All statistical analyses were conducted using GraphPad Prism® 7 or Microsoft Excel 2016.

References

1. Nakane, P.K. and Pierce, G.B. (1966). Enzyme-labeled antibodies: Preparation and application for the localization of antigens. *J. Histochem. Cytochem. 14,* p.929-931
2. Saper, C.B. and Sawchenko, P.E. (2003). Magic peptides, magic antibodies: Guidelines for appropriate controls for immunohistochemistry. *J. Comp. Neurol. 465,* p.161-163
3. Burry, R.W. (2011). Controls for immunocytochemistry: An update. *J. Histochem. Cytochem. 59,* p.6-12
4. Bochtler, T., Löffler, H. and Krämer, A. (2018). Diagnosis and management of metastatic neoplasms with unknown primary. *Semin. Diagn. Pathol. 35,* p.199-206
5. Geramizadeh, B., Marzban, M. and Churg, A. (2016). Role of immunohistochemistry in the diagnosis of solitary fibrous tumor, a review. *Iran J. Pathol. 11,* p.195-203
6. Krajewska, M., Krajwski, S., Epstein, J.I., Shabaik, A., Sauvageot, J., Song, K., Kitada, S. and Reed, J.C. (1996). Immunohistochemical analysis of bcl-2, bax, bcl-X, and mcl-1 expression in prostate cancers. *Am. J. Pathol. 148,* p.1567-1576
7. Guarner, J. and Brandt, M.E. (2011). Histopathologic diagnosis of fungal infections in the 21st century. *Clin. Microbiol. Rev. 24,* p.247-280
8. Haines, D.M. and West, K.H. (2005). Immunohistochemistry: Forging the links between immunology and pathology. *Vet. Immunol. Immunopathol. 108,* p.151-156
9. Eyzaguirre, E. and Hague, A.K. (2008). Application of immunohistochemistry to infections. *Arch. Pathol. Lab Med. 132,* p.424-431
10. Tiniakos, D.G., Brain, J.G. and Bury, Y.A. (2015). Role of histopathology in autoimmune hepatitis. *Dig. Dis. 33,* p.53-64
11. Fujimura, Y. (1996). Pathogenesis of aphtoid ulcers in Crohn's disease: Correlative findings by magnifying colonoscopy, electron microscopy, and immunohistochemistry. *Gut. 38,* p.724-732
12. Larsson, Å., Bredberg, A., Henriksson, G., Manthorpe, R. and Sallmyr, A. (2005). Immunohistochemistry of the B-cell component in lower lip salivary glands of Sjögren's syndrome and healthy subjects. *Scand. J. Immunol. 61,* p.98-107
13. Ehrlich, P. (1877). Contributions to the knowledge of the aniline dyes and their use in the microscopic technique. *Arch. Microsc. Anat. 13,* p.263-278
14. Valent, P., Groner, B., Schumacher, U., Superti-Furga, G., Busslinger, M., Kralovics, R., Zielinski, C., Penninger, J.M., Kerjaschki, D., Stingl, G., Smolen, J.S., Valenta, R., Lassmann, H., Kovar, H., Jäger, U., Kornek, G., Müller, M. and Sörgel, F. (2016). Paul Ehrlich (1854-1915) and his contributions to the foundation and birth of translational medicine. *J. Innate Immun. 8,* p.111-120
15. Behring, E. and Kitasato, S. (1890). Über das zustandekommen der diphtheria-immunität und der tetanus-immunität bei thieren. *Dtsch. Med. Wochenschrift. 49,* p.1113-1114

16. Kaufmann, S.H. (2017). Remembering Emil von Behring: From tetanus treatment to antibody cooperation with phagocytes. *mBio. 8,* e00117-17
17. Childs, G.V. (2014). History of Immunohistochemistry. In: *Pathobiology of human disease.* p.3775-3796
18. Marrack, J. (1934). Nature of antibodies. *Nature. 133,* p.292-293
19. Coons, A.H., Creech, H.J. and Jones, R.N. (1941). Immunological properties of an antibody containing a fluorescent group. *Proc. Soc. Exp. Biol. Med. 47,* p.200-202
20. Vandesande, F. (1979). A critical review of immunocytochemical methods for light microscopy. *J. Neurosci. Methods. 1,* p.3-23
21. Sternberger, L.A. (1969). Some new developmens in immunocytochemistry. *Mikroskopie, 25,* p.346-361
22. Nakane, P.K. and Pierce, G.B. (1967). Enzyme-labeled antibodies for the light and electron microscopic localization of tissue antigens. *J. Cell. Biol. 33,* p.307-318
23. Cotson, S., Holt, S.J. (1958). Studies in enzyme cytochemistry. IV. Kinetics of aerial oxidation of indoxyl and some of its halogen derivatives. *Proc. R. Soc. Lond. B. Biol. Sci. 148,* p.506-519
24. Graham, R.C. and Karnovsky, M.J. (1966). The early stages of absorption of injected horseradish peroxidase in the proximal tubules of mouse kidney: Ultrastructural cytochemistry by a new technique. *J. Histochem. Cytochem. 14,* 291-302
25. Greenwalt, T.J., Swierk, E.M. and Steane, E.A. (1975). Use of horseradish peroxidase-labelled antiglobulin for the colorimetric quantitation of erythrocyte antibodies. *J. Immunol. Methods. 8,* p.351-361
26. Morrell, J.I., Greenberger, L.M. and Pfaff, D.W. (1981). Comparison of horseradish peroxidase visualization methods: Quantitative results and further technical specifics. *J. Histochem. Cytochem. 29,* p.903-916
27. Trojanowski, J.Q., Obrocka, M.A. and Lee, V.M. (1983). A comparison of eight different chromogen protocols for the demonstration of immunoreactive neurofilaments or glial filaments in rat cerebellum using the peroxidase-antiperoxidase method and monoclonal antibodies. *J. Histochem. Cytochem. 31,* p.1217-1223
28. Nakata, T. and Suzuki, N. (2012). Chromogen-based immunohistochemical method for elucidation of the coexpression of two antigens using antibodies from the same species. *J. Histochem. Cytochem. 60,* p.611-619
29. Porstmann, B., Porstmann, T., Nugel, E. and Evers, U. (1985). Which of the commonly used marker enzymes gives the best results in colorimetric and fluorimetric enzyme immunoassays: Horseradish peroxidase, alkaline posphatase or beta-galactosidase? *J. Immunol. Methods. 79,* p.27-37
30. Roberts, I.M., Jones, S.L., Premier, R.R. and Cox, J.C. (1991). A comparison of the sensitivity and specificity of enzyme immunoassays and time-resolved fluoroimmunoassay. *J. Immunol. Methods. 143,* 49-56
31. Kurien, B.T. and Scofield, R.H. (2006). Western blotting. *Methods. 38,* p.283-293

32. Nurjayadi, M., Apriyani, D., Hasan, U., Santoso, I., Kurniadewi, F., Kartika, I.R., Agustini, K., Puspasari, F., Natalia, D. and Mangunwardoyo, W. (2016). Immunogenicity and specificity of anti-recombinant protein Fim-C-*Salmonella typhimurium* antibody as a model to develop Typhoid vaccine. *Procedia Chem. 18,* p.237-245
33. Gräfe, D., Gaitzsch, J., Appelhans, D. and Voit, B. (2014). Cross-linked polymersomes as nanoreactors for controlled and stabilized single and cascade enzymatic reactions. *Nanoscale. 6,* p.10752-10761
34. Chen, J., Zhang, Y., Cheng, M., Guo, Y., Šponer, J., Monchaud, D., Mergny, J-L., Ju, H. and Zhou, J. (2018). How proximal nucleobases regulate the catalytic activity of G-quadruplex/hemin DNAzymes. *ACS Catal. 8,* p.11352-11361
35. Kim, H-S. and Pyun, J-C. (2009). Hyper sensitive strip test with chemiluminescence signal band. *Procedia Chem. 1,* p.1043-1046
36. Ramkiran, A., Mohan, V.G., Mishra, P. and Padmavathy, N. (2018). Enhanced chemiluminescence of luminol by metal peroxides nanoparticles. *Chem. Adv. Mater. 3,* p.16-22
37. Hein, C.D., Liu, X-M, Wang, D. (2008). Click chemistry, a powerful tool for pharmaceutical sciences. *Pharm. Res. 25,* p.2216-2230
38. Sletten, E.M. and Bertozzi, C.R. (2011). From mechanism to mouse: A tale of two biorthogonal reactions. *Acc. Chem. Res. 44,* p.666-676
39. Saxon, E., Armstrong, J.I. and Bertozzi, C.R. (2000). A "traceless" Staudinger ligation for the chemoselective synthesis of amide bonds. *Org. Lett. 2,* p.2141-2143
40. Agard, N.J., Prescher, J.A. and Bertozzi, C.R. (2004). A strain-promoted [3+2] azide-alkyne cycloaddition for covalent modification of biomolecules in living systems. *J. Am. Chem. Soc. 127,* p.15046-15047
41. Kamariza, M., Shieh, P., Faland, C.S., Peters, J.S., Chu, B., Rodriguez-Rivera, F.P., Babu Sait, M.R., Treuren, W.V., Martinson, N., Kalscheuer, R., Kana, B.D. and Bertozzi, C.R. (2018). Rapid detection of *Mycobacterium tuberculosis* in sputum with a solvatochromic trehalose probe. *Sci. Transl. Med. 430,* e.aam6310
42. van Kasteren, S.I., Kramer, H.B., Jensen, H.H., Campbell, S.J., Kirkpatrick, J., Oldham, N.J., Anthony, D.C and Davis, B.G. (2007). Expanding the diversity of chemical protein modification allows post-translational mimicry. *Nature. 446,* p.1105-1109
43. Goddard-Borger, E.D. and Stick, R.V. (2011). An efficient, inexpensive, and shelf-stable diazotransfer reagent: Iamidazole-1-sulfonyl azide hydrochloride. *Org. Lett. 9,* p.3797-3800
44. van Dongen, S.F., Teeuwen, R.L., Nallani, M., van Berkel, S.S., Cornelissen, J.J., Notte, R.J. and van Hest, J.C. (2009). Single-step azide introduction in proteins via an aqueous diazo transfer. *Bioconjug. Chem. 20,* p.20-23
45. Veitch, N.C. (2004). Horseradish peroxidase: A modern view of a classic enzyme. *Phytochemistry. 65,* p.249-259

46. van Hest, J.C.M., Kiick, K.L. and Tirrell, D.A. (2000). Efficient incorporation of unsaturated methionine analogues into proteins *in vivo*. *J. Am. Chem. Soc. 122,* p.1282-1288
47. Dieterich, D.C., Link, A.J., Graumann, J., Tirrell, D.A. and Schuman, E.M. (2006). Selective identification of newly synthesized proteins in mammalian cells using biorthogonal noncanonical amino acid tagging (BONCAT). *Proc. Natl. Acad. Sci. U.S.A. 103,* p.9482-9487
48. Saka, S.K., Wang, Y., Kishi, J.Y., Zhu, A., Zeng, Y., Xie, W., Kirli, K., Yapp, C., Cicconet, M., Beliveau, B.J., Lapan, S.W., Yin, S., Lin, M., Boyden, E.S., Kaeser, P.S., Pihan, G., Church, G.M. and Yin, P. (2019). Immuno-SABER enables highly multiplexed and amplified protein imaging in tissues. *Nat. Biotechnol. 37,* p.1080-1090
49. Bauman, J.E., and Wang, J.C. (1964). Imidazole complexes of nickel (II), copper (II), zinc (II), and silver (I). *Inorg. Chem. 3,* p.368-373
50. Hamada, Y.Z., Cox, R., Hamada, H. (2015). Cu^{2+}-citrate dimer complexes in aqueous solutions. *J. Basic Appl. Sci. 11,* p.583-589
51. Gyliene, O., Vengris, T., Nivinskiene, O. and Binkiene, R. (2010). Decontamination of solutions containing Cu(II) and ligands tartrate, glycine and quadrol using metallic iron. *J. Hazard Mater. 175,* p.452-459
52. Boenisch, T. (2003). Handbook of immunochemical staining methods. 3rd ed. Dako Cytomation Corp., Carpinteria, CA, USA.
53. Radulescu, R.T. and Boenisch, T. (2007). Blocking endogenous peroxidases: A cautionary note for immunohistochemistry. *J. Cell. Mol. Med. 11,* p.1419
54. Adibekian, A., Martin, B.R., Chang, J.W., Hsu, K-L., Tsuboi, K., Bachovchin, D.A., Speers, A.E., Brown, S.J., Spicer, T., Fernandez-Vega, V., Ferguson, J., Hodder, P.S., Rosen, H. and Cravatt, B.F. (2012). Confirming target engagement for reversible inhibitors *in vivo* by kinetically tuned activity-based probes. *J. Am. Chem. Soc. 134,* p.10345-10348
55. van Esbroeck, A.C.M., Janssen, A.P.A., Cognetta, A.B. 3rd, Ogosawara, D., Shpak, G., van der Kroeg, M., Kantae, V., Baggelaar, M.P., de Vrij, F.M.S., Deng, H., Allarà, M., Lin, Z., van der Wel, T., Soethoudt, M., Mock, E.D., den Dulk, H., Baak, I.L., Florea, B.I., Hendriks, G., De Petrocellis, L., Overkleeft, H.S., Hankemeier, T., de Zeeuw, C.I., Di Marzo, V., Maccarone, M., Cravatt, B.F., Kushner, S.A. and van der Stelt, M. (2017). Activity-based protein profiling reveals off-target proteins of the FAAH inhibitor BIA 10-2474. *Science. 356,* p.1084-1087
56. Dana, D., Garcia, J., Bhuiyan, A.I., Rathop, P., Joo, L., Novoa, D.A., Paroly, S., Fath, K.R., Chang, E.J. and Pathak, S.K. (2019). Cell penetrable, clickable and tagless activity-based probe of human cathepsin L. *Bioorg. Chem. 85,* p.505-514
57. Sabidó, E., Tarragó, T., Niessen, S., Cravatt, B.F. and Giralt, E. (2009). Activity-based probes for monitoring post-proline protease activity. *Chembiochem. 10,* p.2361-2366

58. Kato, D., Boatright, K.M. Berger, A.B., Nazif, T., Blum, G., Ryan, C., Chehade, K.A., Salvesen, G.S. and Bogyo. M. (2005). Activity-based probes that target diverse cysteine protease families. *Nat. Chem. Biol. 1,* p.33-38
59. Greenbaum, D., Medzihradszky, K.F., Burlingame, A. and Bogyo, M. (2000). Epoxide electrophiles as activity-dependent cysteine protease profiling and discovery tools. *Chem. Biol. 7,* p.569–581
60. Bachovchin, D.A. and Cravatt, B.F. (2012). The pharmacological landscape and therapeutic potential of serine hydrolases. *Nat. Rev. Drug. Discov. 11,* p.52-68
61. Liu, Y., Patricelli, M.P. and Cravatt. B.F. (1999). Activity-based protein profiling: The serine hydrolases. *Proc. Natl. Acad. Sci. U.S.A. 96,* p.14694–14699.
62. Widen, J.C., Tholen, M., Yim, J.J., Antaris, A., Casey, K.M., Rogalla, S., Klaassen, A., Sorger, J. and Bogyo, M. (2019). Multivariate AND-gate substrate probes as enhanced contrast agents for fluorescence-guided surgery. *BioRxiv,* 695403
63. van Rooden, E.J., Kohsiek, M., Kreekel, R., van Esbroeck, A.C.M., van den Nieuwendijk, A.M.C.H., Janssen, A.P.A., van den Berg, R.J.B.H.N., Overkleeft, H.S. and van der Stelt, M. (2018). Design and synthesis of quenched activity-based probes for diacylglycerol lipase and α,ß-hydrolase domain containing protein. *Chem. Asian. J. 13,* p.3491-3500
64. Deng, H. and van der Stelt, M. (2018). Chemical tools to modulate 2-arachidonoylglycerol biosynthesis. *Biotechnol. Appl. Biochem. 65,* p.9-15
65. Meisslitzer-Ruppitsch, C., Rörhl, C., Neumüller, J., Pavelka, M. and Ellinger, A. (2009). Photooxidation technology for correlated light and electron microscopy. *J. Microsc. 235,* p.322-335
66. Ellisman, M.H., Deerinck, T.J., Shu, X. and Sosinsky, G.E. (2012). Picking faces out of a crowd: Genetic labels for identification of proteins in correlated light and electron microscopy imaging. *Methods Cell. Biol. 111,* p.139-155
67. Rosas-Arellano, A., Villalobos-González, J.B., Palma-Tirado, L., Beltrán, F.A., Cárabez-Trejo, A., Missirlis, F. and Castro, M.A. (2016). A simple solution for antibody signal enhancement in immunofluorescence and triple immunogold assays. *Histochem. Cell. Biol. 146,* p.421-430
68. Jones, L.H., Beal, D., Selby, M.D., Everson, O., Burslem, G.M., Dodd, P., Millbank, J., Tran, T.D., Wakenhut, F., Graham, E.J. and Targett-Adams, P. (2011). In-cell click labelling of small molecules to determine subcellular localisation. *J. Chem. Biol. 4,* p.49-53
69. Potter, G.T., Jayson, G.C., Miller, G.J. and Gardiner, J.M. (2016). An updated synthesis of the diazo-transfer reagent imidazole-1-sylfonyl azide hydrogen sulfate. *J. Org. Chem. 81.* p.3443-3446
70. Hong, V., Presolski, S.I., Ma, C. and Finn, M.G. (2009). Analysis and optimization of copper-catalyzed azide-alkyne cycloaddition for bioconjugation. *Angew. Chem. Int. Ed. Engl. 48,* p.9879-9883

71. Li, N., Lim, R.K., Edwardraja, S. and Lin, Q. (2011). Copper-free Sonogashira cross-coupling for functionalization of alkyne-encoded proteins in aqueous medium and in bacterial cells. *J. Am. Chem. Soc. 133,* p.15316-15319
72. Biagini, S.C.G., Gibsoné, T., Keen, S.E. and Stephen, P. (1998). Cross-metathesis of unsaturated α-amino acid derivatives. *J. Chem. Soc. Perkin Transactions 1, 16,* p.2485-2500
73. Dong, S., Merkel, L., Moroder, L. and Budisa, N. (2008). Convenient syntheses of homopropargylglycine. *J. Pept. Sci. 14,* p.1148-1150
74. Chenault, H.K., Dahmer, J. and Whitesides, G.M. (1989). Kinetic resolution of unnatural and rarely occurring amino acids: Enantioselective hydrolysis of N-acyl amino acids catalyzed by acylase I. *J. Am. Chem. Soc. 111,* p.6354-6364
75. Antoniou, A.N., Blackwood, S.L., Mazzeo, D. and Watts, C. (2000). Control of antigen presentation by single protease cleavage site. *Immunity, 12,* p.391-398
76. Mruk, D.D. and Cheng, C.Y. (2011). Enhanced chemiluminescence (ECL) for routine immunoblotting: An inexpensive alternative to commercially available kits. *Spermatogenesis, 1,* p.121-122